Langmuir

ARTICLE

pubs.acs.org/Langmuir

Graphene as a Spacer to Layer-by-Layer Assemble Electrochemically Functionalized Nanostructures for Molecular Bioelectronic Devices

Xiang Wang,[†] Jingfang Wang,[‡] Hanjun Cheng,[†] Ping Yu,[†] Jianshan Ye,[‡] and Lanqun Mao*,[†]

[†]Beijing National Laboratory for Molecular Sciences, Key Laboratory of Analytical Chemistry for Living Biosystems, Institute of Chemistry, The Chinese Academy of Sciences, Beijing 100190, China

[‡]College of Chemistry and Chemical Engineering, South China University of Technology, Wushan, Guangzhou 510640, China

Supporting Information

ABSTRACT: This study demonstrates the capability of graphene as a spacer to form electrochemically functionalized multilayered nanostructures onto electrodes in a controllable manner through layer-by-layer (LBL) chemistry. Methylene green (MG) and positively charged methylimidazolium-functionalized multiwalled carbon nanotubes (MWNTs) were used as examples of electroactive species and electrochemically useful components for the assembly, respectively. By using graphene as the spacer, the multilayered nanostructures of graphene/MG and graphene/MWNT could be readily formed onto electrodes with the LBL method on the basis of the electrostatic and/or $\pi-\pi$ interaction(s) between graphene and the electrochemically useful components. Scanning electron microscopy (SEM), ultraviolet−visible spectroscopy (UV−vis), and cyclic voltammetry (CV) were used to characterize the assembly processes, and the results revealed that nanostructure assembly was uniform and effective with graphene as the spacer. Electrochemical studies demonstrate that the assembled nanostructures possess excellent electrochemical properties and electrocatalytic activity toward the oxidation of NADH and could thus be used as electronic transducers for bioelectronic devices. This potential was further demonstrated by using an alcohol dehydrogenase-based electrochemical biosensor and glucose dehydrogenase-based glucose/O_2 biofuel cell as typical examples. This study offers a simple route to the controllable formation of graphene-based electrochemically functionalized nanostructures that can be used for the development of molecular bioelectronic devices such as biosensors and biofuel cells.

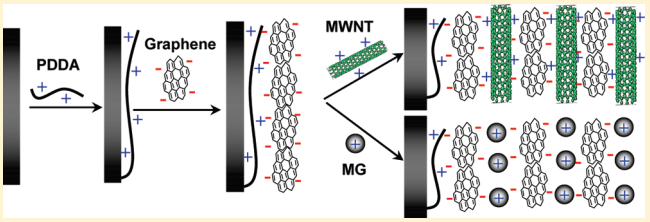

INTRODUCTION

Molecular bioelectronic devices such as biosensors and biofuel cells generally consist of electronic transducers and biorecognition elements.[1] This kind of device has long been one of the central research areas in molecular electronics.[2] Unlike molecular bioelectronics based on the optical coupling of biorecognition elements, the electronic coupling of biorecognition elements with electronic devices requires the efficient transduction of chemical signals generated by the surface-immobilized biorecognition elements into electronic signals. For this purpose, electronic transducers for efficiently transducing biorecognition events into readable electronic signals are generally necessitated in bioelectronic devices. In addition to the requirement for high efficiency and conductivity for electronic transducing, the electronic transducers are often required to have functional structures that can be easily confined to a conducting substrate in a controllable and easily reproducible manner. The latter requirement is of great importance in the fabrication of bioelectronic devices with less device-to-device deviation, which remains very critical when the devices are used for practical applications. Because of their critical importance in molecular bioelectronics, the development of electronic transducers has drawn ever increasing interest, and as a consequence, efficient electronic transducers have been developed.[3]

As one new kind of nanostructure in the carbon family, graphene has unique electronic properties and rich surface chemistry, which are different from those of other kinds of carbon structures such as diamond, fullerene, and carbon nanotubes in the carbon family.[4] The distinct properties of graphene have substantially evoked great interest both in fundamental studies on graphene and in the practical development of many kinds of graphene-based electronic and optical devices such as field-effect transistors,[5] single-electron-transistor circuitry,[6] capacitors,[7] and photovoltaic devices.[8] In addition, the excellent properties of graphene make it very promising in electrochemistry.[9] For example, the high conductivity (i.e., 550 $S \cdot cm^{-1}$)[10] and a large number of electrochemically favorable edge carbons per mass of graphene facilitate electron transfer between molecules to an electrode substrate with a low overpotential.[11] Besides, graphene has a higher specific surface area (i.e., 2630 $m^2 \cdot g^{-1}$) than graphite (i.e., ~10 $m^2 \cdot g^{-1}$) and carbon nanotubes (i.e., 1315 $m^2 \cdot g^{-1}$)[4c,7b] and is envisaged to be useful in the surface immobilization of biomolecules to form functionalized electrode/electrolyte interface for biosensing.[9d−g] Moreover, graphene bears advantages in terms of its easy

Received: October 12, 2010
Revised: July 5, 2011
Published: July 27, 2011

preparation from inexpensive graphite and its good solubility in aqueous media.[12]

Different from the applications mentioned above, this study describes the capability of graphene as a spacer to layer-by-layer assemble electrochemically functionalized nanostructures onto electrodes in a controllable and easily reproducible manner. The assembled functional nanostructures can be used as electronic transducers for molecular bioelectronic devices including electrochemical biosensors and biofuel cells. This capability of graphene is essentially derived from its large conjugative π-electron structure with rich surface chemistry. These properties essentially enable the interactions between graphene and electrochemically active molecules or electrochemically favorable nanostructures and eventually pave a simple route to the controllable formation of electrochemically functionalized nanostructures onto electrodes through layer-by-layer chemistry. Although the interaction of graphene with an electroactive dye, methylene green,[9a] and the LBL assembly of graphene with other kinds of nanostructures have been reported,[9b−d,13] to the best of our knowledge the capability of graphene as a spacer to form electrochemically functional nanostructures that can be used as electronic transducers for bioelectronic devices has not been reported. This study offers an effective approach to the controllable formation of well-ordered functional nanostructures that can be used to transduce biorecognition events efficiently into electronic signals in molecular bioelectronic devices such as biosensors and biofuel cells.

EXPERIMENTAL SECTION

Chemicals and Materials. An aqueous dispersion of graphene was prepared according to previous reports.[14] Briefly, graphite oxide synthesized from graphite by a modified Hummers method was first suspended in water, and the suspension was then subjected to dialysis to remove residual salts and acids. The resulting suspension was again dispersed in water to make a 0.05 wt % dispersion of graphene oxide. The resulting dispersion was subjected to 30 min of centrifugation at 3000 rpm to remove any unexfoliated graphite oxide. After that, 10.0 mL of the aqueous dispersion of exfoliated graphene oxide nanosheets (0.5 mg/mL) was mixed with 10.0 mL of water, 10.0 μL of an aqueous solution of hydrazine (35 wt %), and 70.0 μL of an aqueous solution of ammonia (28 wt %) in a vial, and the resulting mixture was then vigorously stirred for 5 min. The vial was finally put in a water bath (95 °C) for 1 h to produce a stable aqueous dispersion of graphene.

Multiwalled carbon nanotubes (MWNTs, diameter 20−30 nm, length >1 μm) functionalized with positively charged methylimidazolium (MIM) were prepared via procedures reported in our earlier work.[15] Poly(diallydimethylammonium chloride) (PDDA, M_w = 200 000−350 000, 20% aqueous solution) was purchased from Aldrich and used as received. Methylene green (MG) was purchased from Beijing Chemical Company (Beijing, China). Alcohol dehydrogenase (ADH, EC 1.1.1.1, from *Saccharomyces cerevisiae*), glucose dehydrogenase (GDH, EC 1.1.1.47, from *Pseudomonas sp.*), laccase (EC 1.10.3.2, from *Trametes versicolor*), and D-(+)-glucose were all obtained from Sigma. Laccase was purified via a method reported in our early work.[16] Bovine serum albumin (BSA) was obtained from Proliant. Reduced and oxidized forms of nicotinamide adenine dinucleotide (NADH and NAD^+) were purchased from Aldrich. Both multiwalled and single-walled carbon nanotubes (SWNTs, <2 nm in diameter) were purchased from Shenzhen Nanotech Port Co., Ltd. (Shenzhen, China) and purified prior to use. All other chemicals were at least of analytical reagent grade and used as received. Aqueous solutions were prepared with Milli-Q water.

Layer-by-Layer Assembly of Nanostructures with Graphene as a Spacer. Glassy carbon electrodes (GC, 3 mm diameter, Bioanalytical Systems Inc.) were used as the substrate to layer-by-layer assemble the graphene/MG and graphene/MWNT nanostructures. The electrodes were polished first with emery paper and then with aqueous slurries of fine alumina powders (0.3 and 0.05 μm) on a polishing cloth and were finally cleaned with ethanol and Milli-Q water under an ultrasonic bath, each for 5 min. Multilayered nanostructures were assembled on a GC substrate by first immersing the substrate into positively charged PDDA (1 wt % aqueous solution containing 0.5 M NaCl)[17] for 30 min and then cyclically immersing the PDDA-treated substrate into the aqueous dispersion of the negatively charged graphene nanosheets (0.25 mg/mL) and an aqueous solution of the positively charged MG (0.1 mg/mL) or MWNT dispersion for 60 or 30 min, respectively. After each immersion step, the substrate was first carefully rinsed with Milli-Q water to remove the unstably adsorbed materials and then dried with nitrogen gas. For a typical demonstration, the substrate modified with five layers of graphene and MG or MWNTs (hereafter designated as $(graphene/MG)_5$- and $(graphene/MWNT)_5$-modified GC electrodes) are used for the electrochemical measurements and for the fabrication of dehydrogenases-based biosensors and biofuel cells because we found that five layers of graphene and MG have the best electrocatalytic activity toward NADH in terms of the peak current for the electrocatalytic NADH oxidation (Figure S1).

The nanostructure assembly with graphene as a spacer was characterized by scanning electron microscopy (SEM; Hitachi S4800-F microscope, Hitachi Inc., Tokyo, Japan), ultraviolet−visible spectroscopy (UV−vis; UV-1601, Shimadzu, Japan), and cyclic voltammetry (CV; CHI660B, Chenhua, Shanghai, China). $(Graphene/MG)_n$ and $(graphene/MWCNT)_n$ multilayers used for SEM and UV−vis spectroscopic measurements were prepared on an indium tin oxide (ITO)-coated glass plate and a quartz slide, respectively. The ITO-coated glass plate and quartz slide were first cleaned with acetone and then thoroughly rinsed with Milli-Q water. The assembly procedures on the ITO-coated glass plate and quartz slide were performed with the same procedures as those for the GC substrate.

Preparation of the Biosensor and Biofuel Cell. For the preparation of the dehydrogenase-based $(graphene/MG)_5$-modified biosensor and bioanode in the glucose/O_2 biofuel cell with alcohol dehydrogenase (ADH) and glucose dehydrogenase (GDH) as biorecognition elements, respectively, 2 μL of an aqueous solution of ADH or GDH (10 mg/mL) was first mixed with 1 μL of an aqueous solution of BSA (1 wt %) and 1.5 μL of an aqueous solution of glutaraldehyde (1 wt %). The mixture of ADH was then dip-coated onto the $(graphene/MG)_5$-modified GC electrode, and the electrode was allowed to dry at ambient temperature. To prepare the GDH-based bioanode with the $(graphene/MWNT)_5$ nanostructure assembled on the GC electrode, methylene green (MG) used as the electrocatalyst for NADH oxidation was first adsorbed onto the $(graphene/MWNT)_5$ GC electrodes by immersing the electrodes into the aqueous solution of MG (0.01 M) for 30 min and then rinsing the electrodes with water to remove the loosely adsorbed MG. After that, GDH was immobilized onto the MG/$(graphene/MWNT)_5$-modified electrodes to form the bioanode for glucose oxidation using the same procedures described above. To prepare the laccase-based biocathode, 2 μL of the SWNT dispersion in *N,N*-dimethylformamide (1 mg/mL) was dip coated onto the GC electrode and the electrode was dried at ambient temperature. The biocathode was then prepared by cross-linking laccase (2 μL) with BSA (1 μL, 1 wt %) and glutaraldehyde (1.5 μL, 1 wt %) on the SWNT-modified electrode. The electrode was dried at ambient temperature.

Electrochemical Measurements. Electrochemical measurements were carried out in a conventional electrochemical cell with modified GC electrodes as the working electrodes, a platinum wire as the counter electrode, and an Ag/AgCl electrode (KCl-saturated) as the

Scheme 1. Schematic Illustration of the Strategies for the Controllable Formation of Electrochemically Functional Nanostructures on Electrodes with Graphene as the Spacer

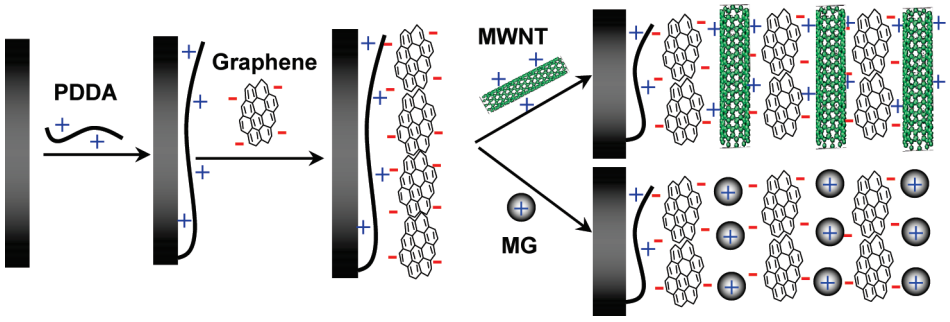

reference electrode. Chronoamperometry used for the study of the properties of the alcohol biosensor was carried out in 0.10 M phosphate buffer (pH 7.0) containing 10 mM NAD^+ with ADH/$(graphene/MG)_5$-modified GC electrodes as the working electrodes under magnetic stirring . The glucose/O_2 biofuel cell (BFC) was assembled by immersing the prepared GDH/MG/$(graphene/MWNTs)_5$-based bioanodes and the laccase-based biocathode into 0.10 M phosphate buffer (pH 6.0) containing 40 mM glucose and 10 mM NAD^+, and the cell performance was evaluated at ambient temperature.

RESULTS AND DISCUSSION

Layer-by-Layer Assembly of Nanostructures with Graphene as a Spacer. To demonstrate the capability of graphene as the spacer to form electrochemically functionalized nanostructures on electrodes through layer-by-layer chemistry, methylene green and carbon nanotubes (CNTs) were employed as typical examples of electrochemically useful components that can be assembled into multilayered nanostructures in a controllable manner, as typically demonstrated in Scheme 1. As one kind of redox dye, MG has been widely used as the electrocatalyst or mediator in electrochemistry and electroanalytical chemistry.[18] In addition, the unique electronic structures and excellent surface chemistry of carbon nanotubes have enabled them to be very promising both in the fundamental electrochemical studies and in the electroanalytical applications.[19] The good electrochemical properties of MG and CNTs have made them particularly attractive in the development of molecular bioelectronic devices such as biosensors and biofuel cells, in which each of them has to be confined to an electrode surface to meet the requirement of the development of integrated bioelectronic devices. Although some methods such as physical adsorption[18] and electropolymerization[20] have been reported for the surface confinement of MG and dip coating has often been employed for the surface immobilization of CNTs,[19a] a method that can assemble these electrochemically useful components into nanostructures onto an electrode surface in a controllable and easily reproducible manner is highly desired for the development of practically applicable molecular bioelectronic devices.

The use of graphene as the spacer to assemble MG molecules onto an electrode surface through layer-by-layer chemistry was essentially based on the electrostatic and/or $\pi-\pi$ stacking interaction(s) between MG and graphene, according to previous reports.[9a,17b] In separate experiments on the UV−vis spectra of MG, graphene, and one layer of MG/graphene on a quartz slide (Figure S2), we found that MG exhibits a strong absorbance at 611 nm and a shoulder at 664 nm, characteristic of the adsorption of the dimer and monomer of MG, respectively.[9a] Graphene nanosheets exhibit a strong absorption at 270 nm, which was attributed to the $\pi \rightarrow \pi^*$ transition of aromatic C═C bonds, indicative of a large π-conjugation network within the reduced graphene nanosheets.[4a,21] The interaction between MG molecules and graphene was presumably evident from the spectrum of the one layer of MG/graphene in which the peak at 611 nm of the MG dimer was red shifted to 638 nm in the graphene/MG layer. This large bathochromic shift (27 nm) suggests that electrostatic and/or $\pi-\pi$ stacking interaction(s) may exist between MG and graphene nanosheets.[22] Such interactions eventually enable graphene as the spacer for the LBL assembly of MG to form a well-structured graphene/MG multilayered nanostructure, as was evident from the changes in the SEM image, UV−vis spectra, and voltammograms obtained for the assembled $(graphene/MG)_n$ multilayers, as depicted in Figure 1. The SEM profiles of the as-assembled $(graphene/MG)_n$ nanostructures demonstrate that an obvious increase in graphene coverage was observed upon repeating the assembly procedures. These demonstrations reveal that through the use of graphene as the spacer a structurally uniform graphene/MG multilayer was readily obtained by the LBL method. As typically shown in Figure 1A, upon assembly for five bilayers of graphene/MG, the crumpled graphene spacers were well interconnected to each other at the edges with small detectable gaps over a microsized range, forming a well-structured conducting graphene/MG network.

The nanostructure assembly with graphene as the spacer was monitored by UV−vis spectroscopy upon assembly of MG with graphene in each bilayer on the quartz slide, as depicted in Figure 1B. PDDA does not exhibit an absorbance at the wavelength employed, whereas the $(graphene/MG)_n$ multilayers show a well-defined peak at 273 nm and two overlapped peaks at ca. 638 nm. The former peak was ascribed to the absorption of both graphene nanosheets and MG molecules, and the latter ones were assigned to the absorption of MG molecules.[9a] The absorbance at 638 nm was found to increase linearly with increasing bilayer numbers (inset in Figure 1B), suggesting the uniform assembly of MG molecules with the graphene spacer in the as-formed layered nanostructure with the LBL method employed in this study. The assembly of MG with graphene as the spacer onto an electrode surface was also characterized by cyclic voltammetry, as depicted in Figure 1C. In 0.10 M phosphate buffer (pH 6.0), two redox waves were observed for

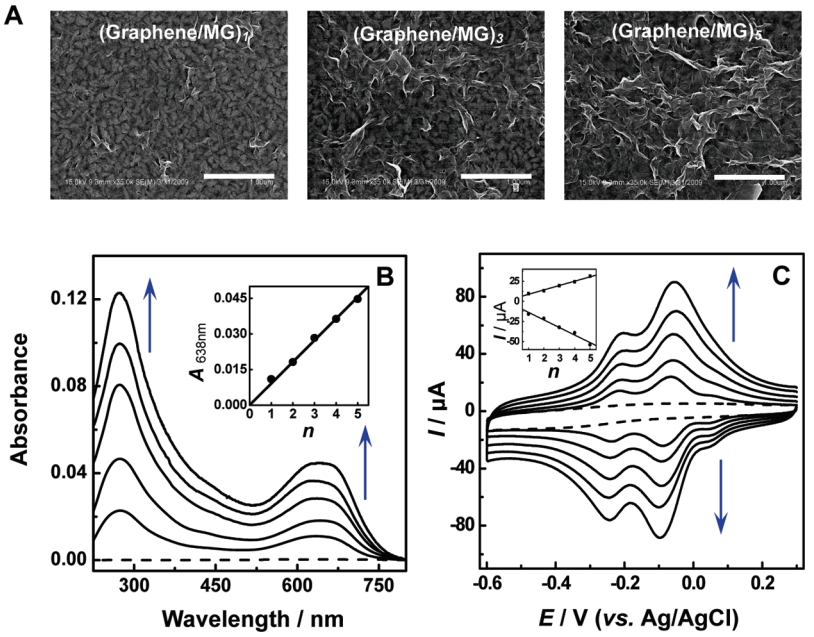

Figure 1. (A) Typical SEM images, (B) UV−vis spectra, and (C) cyclic voltammograms (CVs) for $(graphene/MG)_n$ layer-by-layer assembled onto ITO, quartz slide, and GC electrode, respectively. The scale bar in (A) is 1 μm. Potential scan rate in (C) is100 mV/s. (Inset of B) Plot of the absorbance at 638 nm ($A_{638\ nm}$) versus the number (n) of graphene/MG bilayers. (Inset of C) Anodic (■) and cathodic (●) peak currents of the $(graphene/MG)_n$ nanostructures assembled onto GC electrodes at −0.21 and −0.10 V, respectively, vs the bilayer number (n). The dashed curve in B represents the UV−vis absorbance for the PDDA-modified quartz slide. The dashed curve in (C) represents the CV of graphene-modified GC electrode.

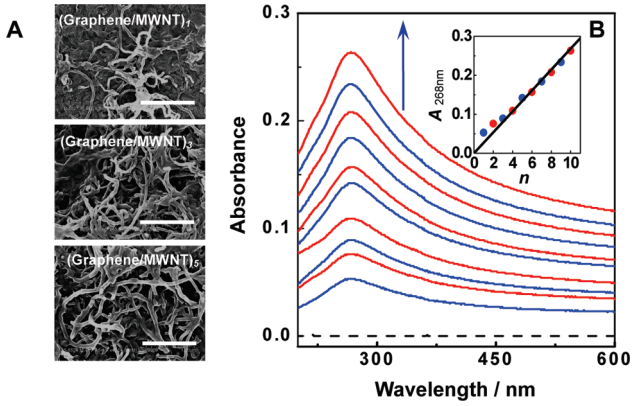

Figure 2. (A) Typical SEM images and (B) UV−vis spectra for $(graphene/MWNT)_n$ assembled layer-by-layer onto ITO and a quartz slide, respectively. The scale bar in A is 1 μm. (Inset of B) Plot of the absorbance at about 268 nm ($A_{268\ nm}$) versus the layer number (n) of graphene (blue) and MWNTs (red). The dashed curve represents the UV−vis absorbance for the PDDA-modified quartz slide.

the layered graphene/MG nanostructures at the formal potentials of −0.08 and −0.23 V, which were ascribed to the redox processes of MG assembled onto graphene nanosheets.[18b] The anodic and cathodic peak currents of the redox peaks at −0.21 and −0.10 V increase linearly with increasing bilayer number (inset, Figure 1C), but the potentials for MG were almost unchanged. These demonstrations reveal that MG, on one hand, was assembled with the graphene nanosheets to form the layered nanostructures and, on the other hand, well maintained its electrochemical properties in the as-assembled nanostructure.

For controllably assembling MWNTs onto an electrode surface with graphene as the spacer, the MWNTs were first functionalized with methylimidazolium moieties to create positive charges on the nanotube surface, enabling the electrostatic interaction between MWNTs and the graphene spacer and, as such, the layer-by-layer assembly of graphene/MWNT multilayered nanostructure. SEM images (Figure 2A) obtained for the graphene/MWNT multilayers reveal an obvious increase in the surface coverage of graphene and MWNTs upon increasing the amount of layer-by-layer assembly, indicating that the use of graphene as the spacer to conduct the stepwise assembly of graphene and MWNT nanostructures essentially produces a homogeneous, porous, 3D graphene/MWNT multilayered nanostructure. Compared with the methods reported for the formation of graphene/CNT hybrids,[23] the strategy demonstrated here by using graphene as the spacer to assemble with positively charged MWNTs might be more effective because of more positive charges created on the nanotube surface through the covalent functionalization of nanotubes with the MIM moiety and the cation−π interaction between methylimidazolium moieties and graphene. As typically shown in the SEM image for $(graphene/MWNT)_5$, crumpled graphene interconnected with the MWNTs and could form an entangled network with a large surface area, which was favorable to the adsorption of redox dyes and the immobilization of enzymes. These properties, along with good conductivity, make the assembled nanostructures very promising for the development of bioelectronic devices.

The graphene/MWNT nanostructure assembly with graphene as the spacer was also monitored by UV−vis spectroscopy upon assembly of MWNTs with graphene in each bilayer on the quartz slide, as depicted in Figure 2B. The spectra of carbon nanostructures exhibit a strong adsorption at around 268 nm, which was attributed to the $\pi \rightarrow \pi^*$ transition of aromatic C=C bonds, indicative of a large π-conjugation network within the reduced graphene and MWNTs.[21] The clear increase in the adsorption at around 268 nm was found upon increasing the

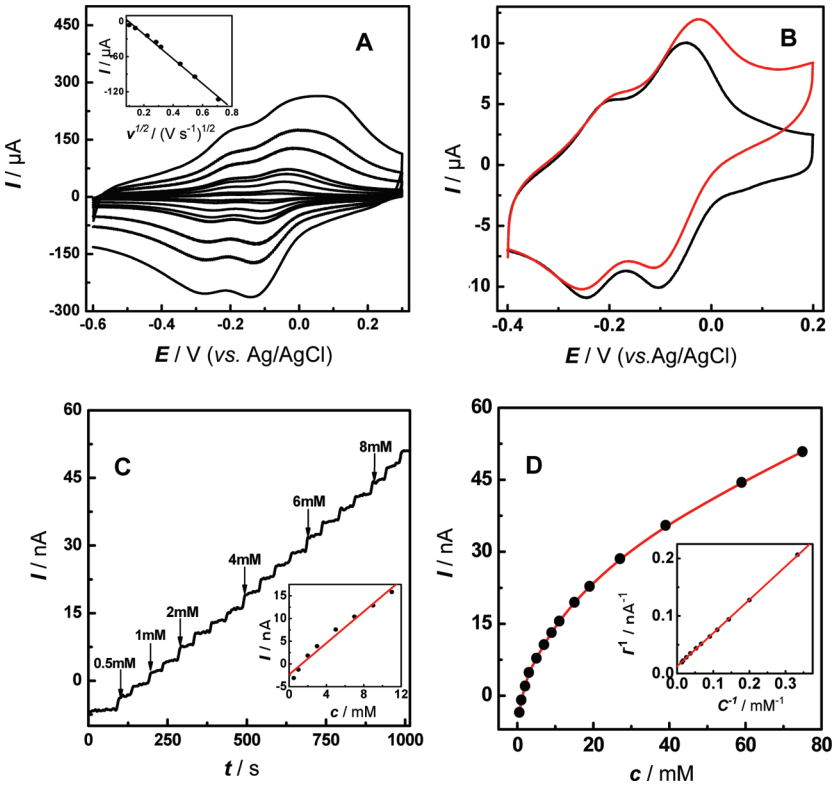

Figure 3. (A) Cyclic voltammograms (CVs) of $(graphene/MG)_5$ multilayer films assembled on a GC electrode in 0.10 M phosphate buffer (pH 6.0) with different scan rates of (from inner to outer) 10, 20, 50, 80, 100, 200, 300, and 500 mV s^{-1}. (Inset) Plot of cathodic peak currents at −0.10 V vs the square root of the potential scan rate. (B) CVs of the $(graphene/MG)_5$-modified GC electrode in 0.10 M phosphate buffer (pH 6.0) in the absence (black curve) and presence (red curve) of 2 mM NADH. Scan rate, 10 mV s^{-1}. (C) Typical current responses of the ADH/$(graphene/MG)_5$-based alcohol biosensor in 0.10 M phosphate buffer (pH 7.0) containing 10 mM NAD^+ under magnetic stirring. The arrows indicate the successive addition of ethanol to the solution. The electrode was polarized at +0.10 V. (Inset) Linear range for alcohol biosensing. (D) Plot of the current responses vs concentration of glucose. (Inset) Lineweaver−Burk plot.

number of layers of graphene and MWNTs (inset, Figure 2B), demonstrating the effective assembly of electrochemically usefully MWNTs with graphene as the spacer.

Toward Electronic Transducing for Molecular Bioelectronic Devices. Figure 3A depicts CVs of $(graphene/MG)_5$ assembled onto a GC electrode in phosphate buffer at various scan rates. The cathodic peak current at −0.13 V varies linearly with the square root of the potential scan rate in the range from 10 to 500 mV s^{-1} (inset), indicating that the redox process of MG assembled into the nanostructures was diffusion-controlled. Moreover, the layered graphene/MG nanostructure assembled onto the GC electrode was relatively stable; the peak currents obtained at the $(graphene/MG)_5$-modified electrode remain stable upon continuously cycling the electrode in the phosphate buffer within a potential range from −0.50 to +0.30 V for at least 50 cycles (Figure S3). In addition, the assembled graphene/MG multilayered nanostructure possesses excellent electrocatalytic activity toward the oxidation of NADH, as shown in Figure 3B. At the $(graphene/MG)_5$-modified electrode, the oxidation of NADH commences at ca. −0.10 V. This potential was more negative than those for NADH oxidation at a bare GC electrode (i.e., +0.70 V under the present conditions)[24] and was comparable to that at an MG/SWNT-modified electrode.[18b] The good electrochemical properties, high stability, and excellent electrocatalytic activity of the assembled graphene/MG multilayered nanostructure with graphene as the spacer eventually make it competent as the electronic transducer for developing biosensors. For example, upon cross-linking alcohol dehydrogenase onto the surface of the graphene/MG multilayered nanostructure assembled on a GC electrode to prepare an alcohol biosensor, the biosensor exhibits a well-defined current response toward the successive addition of alcohol to the solution when the biosensor is polarized at a constant potential of +0.10 V, suggesting that the biosensor with the graphene/MG multilayered nanostructure as the transducer is very responsive. The current response varies linearly with the concentration of alcohol within a concentration range from 0.5 to 11.0 mM with a correlation coefficient of 0.988 (inset, Figure 3C). The sensitivity of the biosensor, measured as the slope of the linear plot, was 24.7 nA $mM^{-1}cm^{-2}$. The apparent Michaelis−Menten constant (K'_m) was calculated according to the Lineweaver−Burk equation[25]

$$\frac{1}{I} = \frac{K'_m}{I_{max}} \times \frac{1}{c} + \frac{1}{I_{max}}$$

where K'_m is the apparent Michaelis−Menten constant, I_{max} represents the maximum current, c is the substrate concentration (i.e., alcohol), and I is the steady current response obtained for each concentration of alcohol. From the Lineweaver−Burk plot (inset, Figure 3D), K'_m was calculated to be 45.8 mM, which was close to the literature value,[26] presumably suggesting that ADH used as a biorecognition element

dx.doi.org/10.1021/la202018r |*Langmuir* 2011, 27, 11180–11186

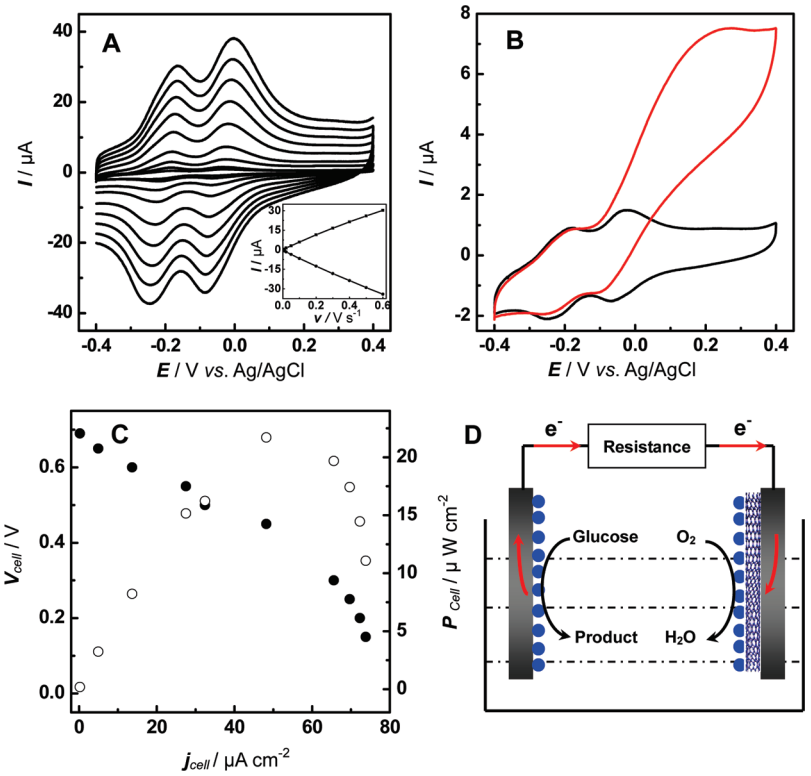

Figure 4. (A) CVs obtained at the MG/(graphene/MWNT)$_5$-modified GC electrode in 0.10 M phosphate buffer (pH 6.0) with different scan rates of (from inner to outer) 10, 50, 100, 200, 300, 400, 500, and 600 mV s^{-1}. (Inset) Plot of cathodic peak currents (●) measured at −0.08 V and anodic peak currents (■) measured at −0.17 V vs the potential scan rate. (B) CVs of the MG/(graphene/MWNT)$_5$-modified GC electrode in 0.10 M phosphate buffer (pH 6.0) in the absence (black curve) and presence (red curve) of 2 mM NADH in the buffer. The scan rate is 20 mV s^{-1}. (C) Polarization curve (●) of the assembled glucose/O_2 biofuel cell and the dependence of the power output (○) on the current density in the quiescent phosphate buffer (0.10 M, pH 6.0) containing 10 mM NAD^+ and 30 mM glucose under ambient air. (D) Schematic depiction of the glucose/O_2 biofuel cell.

retained its native secondary conformational structure on the as-assembled graphene/MG electronic transducer.

Figure 4A depicts CVs of the MG/(graphene/MWNT)$_5$-modified electrode in 0.10 M phosphate buffer (pH 6.0) at different scan rates. Both the cathodic peak current at −0.08 V and the anodic peak current at −0.17 V vary linearly with the potential scan rate in the range employed here (inset), indicating that the redox process of MG confined to the graphene/MWNT nanostructures was a surface-controlled process that was different from that of MG assembled into the nanostructure with graphene as the spacer. This difference can be elucidated as follows. Because the redox process of MG is pH-dependent, the diffusion of H^+ in the multilayers of graphene/MG will control the redox process as the scan rate increases.[18c] These properties eventually result in a diffusion-controlled process of MG in (graphene/MG)$_5$ (Figure 3A). However, when MG is adsorbed on the surface of (graphene/MWNT)$_5$ multilayers, H^+ in the buffer solution can easily participate in the redox process of MG and, as a result, the redox process of MG confined to (graphene/MWNT)$_5$ becomes surface-controlled (Figure 4A). Moreover, the MG/(graphene/MWNTs)$_5$-modified electrode also possesses excellent electrocatalytic activity toward the oxidation of NADH (Figure 4B), resulting in a low potential for NADH oxidation. These properties substantially enabled the as-assembled graphene/MWNT multilayered nanostructures to be the electronic transducer for bioelectronic devices upon the absorption of the MG electrocatalyst. For instance, the prepared MG/(graphene/MWNTs)$_5$ confined to the GC electrode were further developed as the bioanode for glucose oxidation after the immobilization of glucose dehydrogenase on the electrode surface. After being assembled with the laccase-based biocathode to form a glucose/O_2 biofuel cell, the cell has an open-circuit voltage of 0.69 V and a maximum power density of 22.50 μW cm^{-2} at 0.48 V in the quiescent phosphate buffer (0.10 M, pH 6.0) containing 10 mM NAD^+ and 30 mM glucose under ambient air (Figure 4C). These values are comparable to those of the enzymatic BFCs reported in literature,[24] demonstrating that the use of graphene as the spacer to form the multilayered nanostructure in a controllable manner offers a new approach to the development of electrochemically functionalized nanostructures that can be used as electronic transducers for bioanodes in enzymatic biofuel cells.

CONCLUSIONS

We have demonstrated the capability of graphene as the spacer to assemble electrochemically functionalized nanostructures onto electrodes with layer-by-layer chemistry in a controllable and easily reproducible manner. The assembled nanostructures possess advantages, such as excellent electrocatalytic activity, high conductivity, and high surface area, benefitting both from the electroactive or electrochemically useful components and from the graphene spacer. These properties allow the graphene-based multilayered nanostructures to serve as electronic transducers for molecular bioelectronic devices such as biosensors and biofuel cells. This study essentially allows a simple, controllable

approach to the development of electrochemically useful nanostructures with promising applications in the future development of molecular bioelectronic devices such as biosensors and biofuel cells.

■ ASSOCIATED CONTENT

Supporting Information. CVs for the oxidation of NADH at different $(graphene/MG)_n$-modified GC electrodes. UV−vis spectra of MG, graphene, and $(graphene/MG)_1$. Stability of the $(graphene/MG)_5$-modified electrode. This material is available free of charge via the Internet at http://pubs.acs.org.

■ AUTHOR INFORMATION

Corresponding Author
*Fax: +86-10-62559373. E-mail: lqmao@iccas.ac.cn.

■ ACKNOWLEDGMENT

This work was financially supported by the NSF of China (grant nos. 90813032, 20975104, and 20935005 for L.M. and 20805050 for P.Y.), the National Basic Research Program of China (973 Program, 2007CB935603 and 2010CB933502), and the Chinese Academy of Sciences (KJCX2-YW-W25 and Y2010015).

■ REFERENCES

(1) (a) Scheller, F. W.; Wollenberger, U. In *Bioelectrochemistry*; Wilson, G. S., Ed.; Wiley-VCH: Weinheim, 2002; Chapter 13, p 431. (b) Heller, A.; Degani, Y. In *Redox Chemistry and Interfacial Behavior of Biological Molecules*; Dryhurst, G., Niki, K., Eds.; Plenum: New York, 1988; Chapter 11, p 151. (c) Katakis, I.; Heller, A. In *Frontiers in Biosensorics I: Fundamental Aspects*; Scheller, F. W., Schubert, F., Fedrowitz, J., Eds.; Birkhäuser Verlag: Basel, 1997; p 220. (d) Willner, I.; Katz, E. In *Bioelectronics: From Theory to Applications*; Willner, I., Katz, E., Eds.; Wiley-VCH: Weinheim, 2005; Chapter 1, p 1.

(2) (a) Jia, W.; Wang, K.; Zhu, Z.; Song, H.; Xia, X. *Langmuir* **2007**, *23*, 11896. (b) Bharathi, S.; Nogami, M.; Lev, O. *Langmuir* **2001**, *17*, 2602. (c) Li, Y.; Neoh, K. G.; Cen, L.; Kang, E. T. *Langmuir* **2005**, *21*, 10702. (d) Rubio-Retama, J.; Hernando, J.; López-Ruiz, B.; Härtl, A.; Steinmüller, D.; Stutzmann, M.; López-Cabarcos, E.; Garrido, J. A. *Langmuir* **2006**, *22*, 5837. (e) White, R. J.; Phares, N.; Lubin, A. A.; Xiao, Y.; Plaxco, K. W. *Langmuir* **2008**, *24*, 10513. (f) Li, X.; Zhou, Y.; Zheng, Z.; Yue, X.; Dai, Z.; Liu, S.; Tang, Z. *Langmuir* **2009**, *25*, 6580. (g) Zhou, H.; Zhang, Z.; Yu, P.; Su, L.; Ohsaka, T.; Mao, L. *Langmuir* **2010**, *26*, 6028.

(3) (a) Lu, Y.; Li, X.; Zhang, L.; Yu, P.; Su, L.; Mao, L. *Anal. Chem.* **2008**, *80*, 1883. (b) Yan, J.; Zhou, H.; Yu, P.; Su, L.; Mao, L. *Adv. Mater.* **2008**, *20*, 2899. (c) Misra, N.; Martinez, J. A.; Huang, S.; Wang, Y.; Stroeve, P.; Grigoropoulos, C.; Noy, A. *Proc. Natl. Acad. Sci. U.S.A.* **2009**, *106*, 13780. (d) Xiang, Y.; Xie, M.; Bash, R.; Chen, J.; Wang, J. *Angew. Chem., Int. Ed.* **2007**, *46*, 9054. (e) Cohen-Karni, T.; Qing, Q.; Li, Q.; Fang, Y.; Lieber, C. M. *Nano Lett.* **2010**, *10*, 1098.

(4) (a) Li, D.; Muller, M. B.; Gilje, S.; Kaner, R. B.; Wallace, G. G. *Nat. Nanotechnol.* **2008**, *3*, 101. (b) Li, D.; Kaner, R. B. *Science* **2008**, *320*, 1170. (c) Geim, A. K.; Novoselov, K. S. *Nat. Mater.* **2007**, *6*, 183.

(5) Li, X.; Wang, X.; Zhang, L.; Lee, S.; Dai, H. *Science* **2008**, *319*, 1229.

(6) Li, X.; Cai, W.; An, J.; Kim, S.; Nah, J.; Yang, D.; Piner, R.; Velamakanni, A.; Jung, I.; Tutuc, E.; Banerjee, S. K.; Colombo, L.; Ruoff, R. S. *Science* **2009**, *324*, 1312.

(7) (a) Yu, D.; Dai, L. *J. Phys. Chem. Lett.* **2010**, *1*, 467. (b) Stoller, M.; Park, S.; Zhu, Y.; An, J.; Ruoff, R. S. *Nano Lett.* **2008**, *8*, 3498.

(8) Williams, G.; Kamat, P. V. *Langmuir* **2009**, *25*, 13869.

(9) (a) Liu, H.; Gao, J.; Xue, M.; Zhu, N.; Zhang, M.; Cao, T. *Langmuir* **2009**, *25*, 12006. (b) Wang, D.; Wang, X. *Langmuir* **2011**, *27*, 2007. (c) Zeng, G. H.; Xing, Y. B.; Gao, J. A.; Wang, Z. Q.; Zhang, X. *Langmuir* **2010**, *26*, 15022. (d) Shan, C.; Yang, H.; Han, D.; Zhang, Q.; Ivaska, A.; Niu, L. *Langmuir* **2009**, *25*, 12030. (e) Zuo, X. L.; He, S. J.; Li, D.; Peng, C.; Huang, Q.; Song, S. P.; Fan, C. H. *Langmuir* **2010**, *26*, 1936. (f) Zhou, M.; Zhai, Y. M.; Dong, S. J. *Anal. Chem.* **2009**, *81*, 5603. (g) Tang, L.; Wang, Y.; Li, Y.; Feng, H. B.; Lu, J.; Li, J. *Adv. Funct. Mater.* **2009**, *19*, 2782.

(10) Wang, X.; Zhi, L.; Müllen, K. *Nano Lett.* **2008**, *8*, 323.

(11) Ambrosi, A.; Bonanni, A.; Pumera, M. *Nanoscale* **2011**, *3*, 2256.

(12) Stankovich, S.; Dikin, D. A.; Dommett, G. H. B.; Kohlhaas, K. M.; Zimney, E. J.; Stach, E. A.; Piner, R. D.; Nguyen, S. T.; Ruoff, R. S. *Nature* **2006**, *442*, 282.

(13) (a) Shen, J. F.; Hu, Y. Z.; Li, C.; Qin, C.; Shi, M.; Ye, M. X. *Langmuir* **2009**, *25*, 6122. (b) Liu, J. Q.; Tao, L.; Yang, W. R.; Li, D.; Boyer, C.; Wuhrer, R.; Braet, F.; Davis, T. P. *Langmuir* **2010**, *26*, 10068. (c) Zhu, C. Z.; Guo, S. J.; Zhai, Y. M.; Dong, S. J. *Langmuir* **2010**, *26*, 7614.

(14) (a) Kovtyukhova, N. I.; Ollivier, P. J.; Martin, B. R.; Mallouk, T. E.; Chizhik, S. A.; Buzaneva, E. V.; Gorchinskiy, A. D. *Chem. Mater.* **1999**, *11*, 771. (b) Hummers, W.; Offeman, R. *J. Am. Chem. Soc.* **1958**, *80*, 1339.

(15) Xiang, L.; Zhang, Z.; Yu, P.; Zhang, J.; Su, L.; Ohsaka, T.; Mao, L. *Anal. Chem.* **2008**, *80*, 6587.

(16) Zheng, W.; Li, Q.; Su, L.; Yan, Y.; Zhang, J.; Mao, L. *Electroanalysis* **2006**, *18*, 587.

(17) (a) Zhang, M.; Yan, Y.; Gong, K.; Mao, L.; Guo, Z.; Chen, Y. *Langmuir* **2004**, *20*, 8781. (b) Yan, Y.; Zhang, M.; Gong, K.; Su, L.; Guo, Z.; Mao, L. *Chem. Mater.* **2005**, *17*, 3457.

(18) (a) Lin, Y.; Zhu, N.; Yu, P.; Su, L.; Mao, L. *Anal. Chem.* **2009**, *81*, 2067. (b) Li, X.; Zhou, H.; Yu, P.; Su, L.; Ohsaka, T.; Mao, L. *Electrochem. Commun.* **2008**, *10*, 851. (c) Han, J.; Yu, A.; Chen, H. *Acta Chim. Sin.* **1995**, *53*, 362.

(19) (a) Tran, T. O.; Lammert, E. G.; Chen, J.; Merchant, S. A.; Brunski, D. B.; Keay, J. C.; Johnson, M. B.; Glatzhofer, D. T.; Schmidtke, D. W. *Langmuir* **2011**, *27*, 6201. (b) Lee, D.; Cui, T. *Langmuir* **2011**, *27*, 3348. (c) Mantha, S.; Pedrosa, V. A.; Olsen, E. V.; Davis, V. A.; Simonian, A. L. *Langmuir* **2010**, *26*, 19114. (d) Felhofer, J. L.; Caranto, J. D.; Garcia, C. D. *Langmuir* **2010**, *26*, 17178. (e) Yeh, S. R.; Chen, Y. C.; Su, H. C.; Yew, T. R.; Kao, H. H.; Lee, Y. T.; Liu, T. A.; Chen, H.; Chang, Y. C.; Chang, P.; Chen, H. *Langmuir* **2009**, *25*, 7718. (f) Hu, C.; Hu, S. *Langmuir* **2008**, *24*, 8890.

(20) Ulyanova, Y. V.; Blackwell, A. E.; Minteer, S. D. *Analyst* **2006**, *131*, 257.

(21) Clark, B. J.; Frost, T.; Russell, M. A. *UV Spectroscopy: Techniques, Instrumentation, Data Handling/UV Spectrometry Group*; Chapman & Hall: London, 1993; Vol. 4.

(22) Xu, Y.; Zhao, L.; Bai, H.; Hong, W.; Li, C.; Shi, G. *J. Am. Chem. Soc.* **2009**, *131*, 13490.

(23) (a) Kim, Y. K.; Min, D. H. *Langmuir* **2009**, *25*, 11302. (b) Hong, T. K.; Lee, D. W.; Choi, H. J.; Shin, H. S.; Kim, B. S. *ACS Nano* **2010**, *4*, 3861. (c) Yu, D. S.; Dai, L. M. *J. Phys. Chem. Lett.* **2010**, *1*, 467.

(24) Yan, Y.; Zheng, W.; Su, L.; Mao, L. *Adv. Mater.* **2006**, *18*, 2639.

(25) Mell, L. D.; Malloy, J. T. *Anal. Chem.* **1975**, *47*, 299.

(26) Vanni, A.; Anfossi, L.; Pessione, E; Giovannoli, C. *Int. J. Biol. Macromol.* **2002**, *30*, 41.